JOURNAL OF GEOPHYSICAL RESEARCH, VOL. 113, G02007, doi:10.1029/2007JG000476, 2008

Oceanic loading of wildfire-derived organic compounds from a small mountainous river

Glendon B. Hunsinger,[1] Siddhartha Mitra,[1,2] Jonathan A. Warrick,[3] and Clark R. Alexander[4]

Received 30 April 2007; revised 4 December 2007; accepted 21 December 2007; published 11 April 2008.

[1] Small mountainous rivers (SMRs) export substantial amounts of sediment into the world's oceans. The concomitant yield of organic carbon (OC) associated with this class of rivers has also been shown to be significant and compositionally unique. We report here excessively high loadings of polycyclic aromatic hydrocarbons (PAHs), lignin, and levoglucosan, discharged from the Santa Clara River into the Santa Barbara Channel. The abundance of PAHs, levoglucosan, and lignin in Santa Barbara Channel sediments ranged from 201.7 to 1232.3 ng gdw^{-1}, 1.3 to 6.9 μg gdw^{-1}, and 0.3 to 2.2 mg per 100 mg of the sedimentary OC, respectively. Assuming a constant rate of sediment accumulation, the annual fluxes of PAHs, levoglucosan, and lignin, to the Santa Barbara Channel were respectively, 885.5 ± 170.2 ng cm^{-2} a^{-1}, 3.5 ± 1.9 μg cm^{-2} a^{-1} and 1.4 ± 0.3 mg per 100 mg OC cm^{-2} a^{-1}, over ~30 years. The close agreement between PAHs, levoglucosan, and lignin abundance suggests that the depositional flux of these compounds is largely biomass combustion-derived. To that end, use of the Santa Clara River as a model for SMRs suggests this class of rivers may be one of the largest contributors of pyrolyzed carbon to coastal systems and the open ocean. Wildfire associated carbon discharged from other high yield fluvial systems, when considered collectively, may be a significant source of lignin, pyrolytic PAHs, and other pyrogenic compounds to the ocean. Extrapolating these methods over geologic time may offer useful historical information about carbon sequestration and burial in coastal sediments and affect coastal carbon budgets.

Citation: Hunsinger, G. B., S. Mitra, J. A. Warrick, and C. R. Alexander (2008), Oceanic loading of wildfire-derived organic compounds from a small mountainous river, *J. Geophys. Res.*, *113*, G02007, doi:10.1029/2007JG000476.

1. Introduction

[2] Small mountainous rivers (SMRs), as a class of rivers, have been suggested to export substantial amounts of sediment [*Milliman and Syvitski*, 1992] and organic carbon (OC) directly to the global ocean [e.g., *Blair et al.*, 2004]. In many cases, the OC discharged from small mountainous rivers is refractory in composition and composed of fossil petrogenetic OC, contributing to the age of oceanic carbon [*Kao and Liu*, 1996; *Komada et al.*, 2004; *Leithold et al.*, 2006]. However, many small mountainous rivers throughout the world, such as the Eel and Santa Clara Rivers (North America), Aure and Fly Rivers (Papua New Guinea), Cleddau and Hokitika Rivers (New Zealand), and Tsengwen and Lanyang Hsi Rivers (Taiwan) [*Milliman and Syvitski*, 1992], drain watersheds that are subjected to recurring wildfires [e.g., *Hao and Liu*, 1994; *Pyne*, 1997; *Lohman et al.*, 2007]. The occurrence of wildfire results in increased soil erosion and carbon loading to coastal systems [e.g., *Florsheim et al.*, 1991; *Keller et al.*, 1997; *Johansen et al.*, 2001; *Moody and Martin*, 2001; *Lave and Burbank*, 2004; *Rulli and Rosso*, 2005; *Shakesby and Doerr*, 2006]. Furthermore, wildfires consume vegetative ground cover leaving behind ash, char, and burn laden soils rich in condensed macromolecular organic compounds [*Shafizadeh*, 1982; *Evans and Milne*, 1987; *Giovannini and Lucchesi*, 1997; *McGrath et al.*, 2001; *Lynch et al.*, 2004]. Such pyrogenic compounds can be chemically distinguished from refractory petrogenetic OC delivered to coastal systems.

[3] Combustion of biomass can produce a chemical "fingerprint" on the landscape and in receiving waters following erosion events. The heating of soil organic matter (OM) leads to an increase in its aromaticity and removal of oxygen-containing functional groups, while dehydration and decarboxylation transforms OM into an insoluble form, resistant to oxidation and degradation [*Shafizadeh*, 1982; *Evans and Milne*, 1987; *Almendros et al.*, 1990; *McGrath et al.*, 2001; *Gonzalez-Perez et al.*, 2004; *Lynch et al.*, 2004]. Fire temperatures between 100 and 200°C induce loss of soil OM with dehydration and distillation of volatiles

[1]Department of Geological Sciences and Environmental Studies, Binghamton University, Binghamton, New York, USA.
[2]Now at East Carolina University, Department of Geological Sciences, Greenville, North Carolina, USA.
[3]USGS Pacific Science Center, Santa Cruz, California, USA.
[4]Skidaway Institute of Oceanography, Savannah, Georgia, USA.

0148-0227/08/2007JG000476

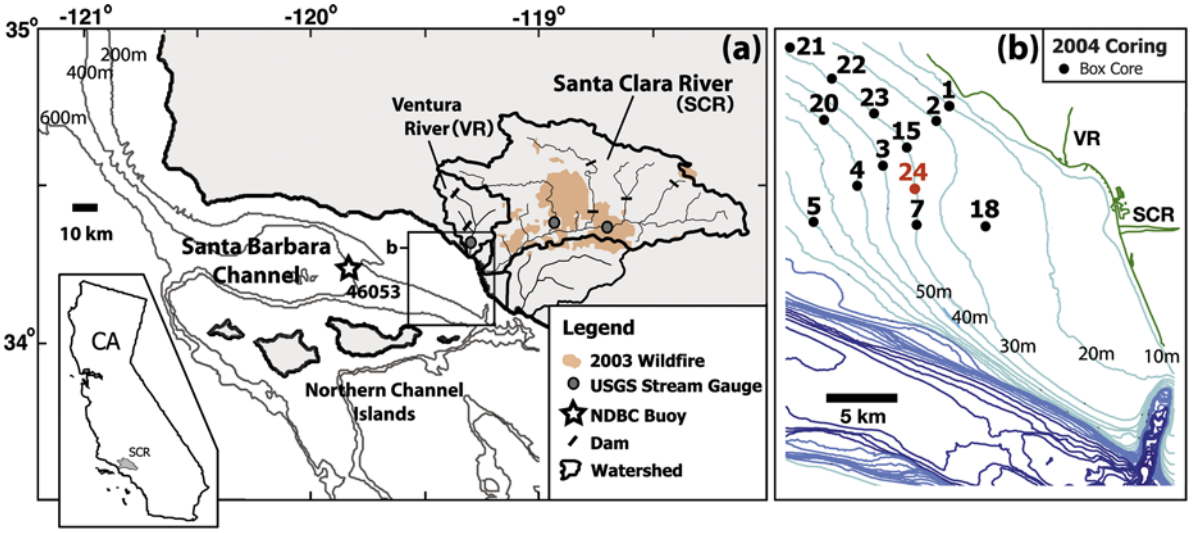

Figure 1. Site locus and sampling map for the Santa Clara Basin and Santa Barbara Channel, California. (a) Regional view of site location; (b) nearshore sampling locations along NE and NW transects highlighting surficial stations (black) and down core station 24 (red). VR = Ventura River, SCR = Santa Clara River.

[*Czimczik et al.*, 2002, 2003]. At higher temperatures, soil OM becomes charred, creating stable carbonaceous residues known as black carbon [*Giovannini and Lucchesi*, 1997; *Czimczik et al.*, 2003]. Furthermore, the combustion of cellulose results in the production of the carbohydrate levoglucosan, lignin phenols, abietanes, and polycyclic aromatic hydrocarbons (PAHs) [*McGrath et al.*, 2001; *Simoneit and Elias*, 2001; *Simoneit*, 2002; *Oros et al.*, 2002; *Otto et al.*, 2006]. Thus, biomass and soil combustion may leave a characteristic suite of organic markers which can be used to track wildfires. Moreover, these compounds, due to their formation mechanisms involving aromatization and condensation, are presumably refractory; that is, they exhibit slow turnover and oxidation back into CO_2(g) [*Giovannini and Lucchesi*, 1997; *Lynch et al.*, 2004].

[4] The watershed of the Santa Clara River in southern California (Figure 1) has been subject to recurrent wildfires with a minimum average annual area of ~65 km^2 (≥2% of

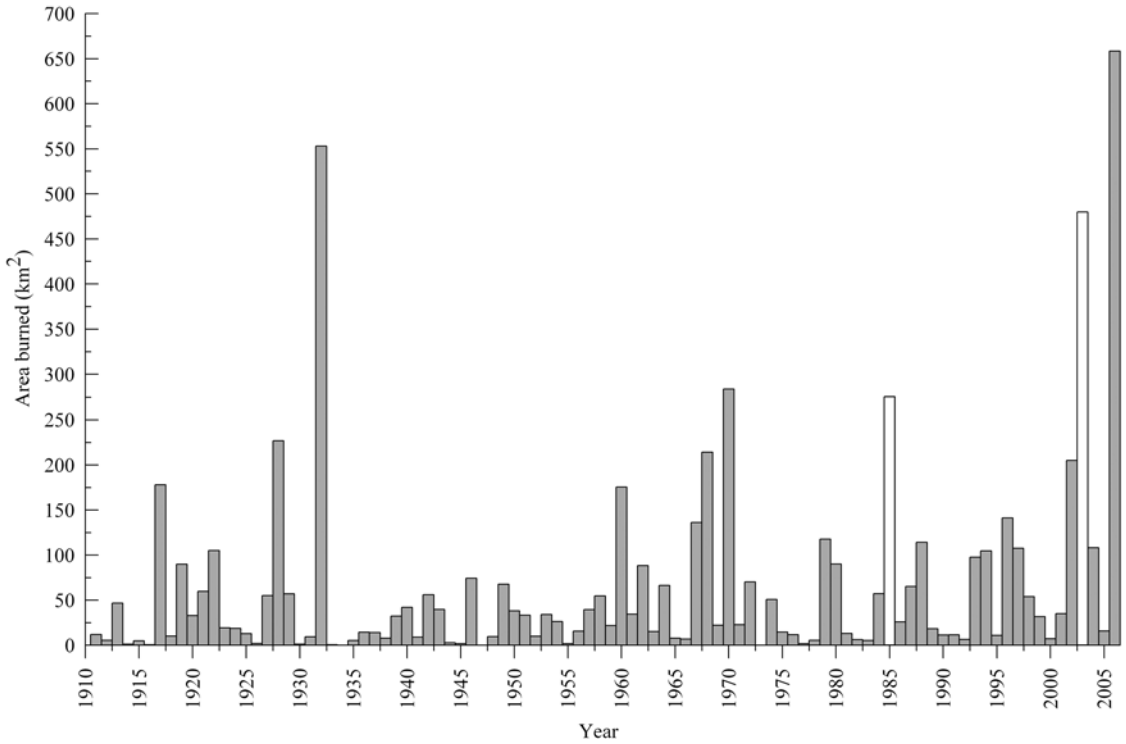

Figure 2. Fire record of the Santa Clara watershed from 1910 until 2006 (CaDFFP http://frap.cdf.ca.gov/data/). Highlighted are the areas burned during the 1985 and 2003 fires.

the watershed's surface area) from 1910 to the present (Figure 2; CaDFFP http://frap.cdf.ca.gov/data/) [e.g., *Pyne*, 1997; *Mensing et al.*, 1999]. Nearly 480 km^2 of the watershed (>11%) succumbed to wildfires from late September to early November 2003 [*Blackwell and Tuttle*, 2004]. These burn events were then followed by extensive rainfall, flooding, and erosion in the winter of 2004. Given the propensity of large scale wildfires in the Santa Clara drainage basin (Figure 2) and the excessive oceanic sediment yield of SMRs [*Milliman and Syvitski*, 1992], we hypothesized that the Santa Clara River may be a substantial contributor of pyrolyzed carbon to the Santa Barbara Channel and that the yield of this material may be important, globally. In that context, the objectives of this study were, 1) to estimate the flux of select biomass and biomass combustion-derived organic compounds into the Santa Barbara Channel, and 2) to compare the sedimentary flux of biomass combustion-derived PAHs in the Santa Barbara Channel to concentrations of sedimentary PAHs in coastal shelf systems globally. To our knowledge, this work is the first attempt to use PAHs signatures in conjunction with other biomarkers to isolate wildfire-derived sediment deposition into the coastal ocean.

2. Site Description

[5] The Santa Clara River originates in the Western Transverse Range of California (Figure 1). Sediment yield from the Western Transverse Range rivers (1500 to 3600 t km^{-2} a^{-1}) is considerably higher than most California coastal rivers due to, 1) weak sedimentary bedrock, 2) active tectonics [*Scott and Williams*, 1978; *Inman and Jenkins*, 1999; *Warrick*, 2002], and 3) extensive erosion of both contemporary and mature soils [*Masiello and Druffel*, 2001; *Komada et al.*, 2004]. This range in sediment yield is also exceedingly high compared to other high, mountainous rivers of the world [*Milliman and Syvitski*, 1992].

[6] The Santa Clara River drains directly into the Santa Barbara Channel (Figure 1) [*Milliman and Syvitski*, 1992; *Warrick et al.*, 2004]. The Santa Clara is the largest watershed (4,210 km^2) and dominant source of sediment to the Santa Barbara Channel (~3.5 to ~6.3 Mt a^{-1}) [*Schwalbach and Gorsline*, 1985; *Warrick*, 2002]. Other river sources include the Ventura River (~1.1 Mt a^{-1}) and the numerous, small drainages (~1.7 Mt a^{-1}) that discharge around the coastline of the channel (Figure 1).

[7] Santa Clara River discharge is driven by episodic winter rainfall, which results in the majority of annual sediment discharge occurring during only 1 to 5 days per year [*Mount*, 1995; *Warrick*, 2002]. Large storms are more likely to occur during ENSO influenced winters as shown by *Inman and Jenkins* [1999] and *Andrews et al.* [2004]. Sediment production from a burned landscape is commonly an order of magnitude higher than unburned landscape, due to post-fire dry ravel, rilling, gullying and mass wasting [*Keller et al.*, 1997; *Lave and Burbank*, 2004; *Rulli and Rosso*, 2005]. Thus, wildfires such as those that occur regularly in the Santa Clara watershed (e.g., Figure 2) will substantially increase both water and sediment discharge from southern California landscapes, especially during the first winter storm following the burn [*Florsheim et al.*, 1991; *Lave and Burbank*, 2004; *Warrick and Rubin*, 2007].

[8] Suspended sediment within the Santa Clara River basin is derived from a number of sources. Analysis of bulk carbon, nitrogen and isotopic signatures of particulate organic carbon from the Santa Clara watershed indicates mixing of bedrock and heavily weathered soils [*Masiello and Druffel*, 2001; *Komada et al.*, 2004]. Most of the watershed (88%) is native chaparral or woodland (oak and pine), while the remaining area is represented by agriculture (4.2%), urban (3.1%), barren (2.7%) and grassland (2.0%) [*Warrick*, 2002]. The limited agricultural and urban inputs are concentrated along the long, east–west running main stem river channel and near the river mouth (Figure 1). As such, the dominant source of particulate carbon in this system is allocthonous, while autocthonous sources are inherently low.

[9] Sediment from the Santa Clara accounts for approximately 85% of the Santa Barbara Basin sediment mass [*Schwalbach and Gorsline*, 1985] and almost all of the Ventura Shelf sediment [*Dahlen et al.*, 1990]. The vast majority of river sediment discharged into the Santa Barbara Channel settles from the buoyant freshwater plume within 1 km of the coastline [*Mertes and Warrick*, 2001; *Warrick et al.*, 2004]. This results from rapid settling via flocculation, convective instabilities, and/or negative buoyancy due to the exceptionally high river sediment concentrations ($\geq$10 g L^{-1}) as reported by *Warrick and Milliman* [2003]. As an example, the majority of river sediment discharged into the channel settled immediately on the inner (~50m depth) shelf following the large 1969 fire and flooding events [*Drake et al.*, 1972]. Once on the seabed, sediment is redistributed by bottom boundary layer processes, which likely include both dilute suspended and dense fluid mud transport that distribute the sediment offshore to the outer shelf and basin [*Kolpack and Drake*, 1984]. *Alexander et al.* [2008] estimate that approximately 20% of the river's annual sediment discharge is retained on the shelf over 100-yr timescales.

3. Methods

3.1. Sampling

[10] Surface sediment grab samples and sediment cores up to 38 cm in depth were collected shipboard from the modern Santa Clara river plume depositional zone [*Warrick et al.*, 2004] on 12, 13, and 15 March 2004 (Figure 1). These cruises were conducted following extensive wildfires of October 2003 and watershed-wide rainfall events which occurred in the late winter of 2004, from the 2nd to 5th of February and from the 22nd of February to the 5th of March. Thus, sediment sampling at that time period was ideal for evaluating the flux of pyrolyzed carbon into the Santa Barbara Channel due to watershed-wide wildfires.

[11] Two cruise transects were completed, one along a north-west, and another along a north-east trend. The goal of this sampling strategy was to collect sediments along a coastline transect at consistent water depth of ~40 m and perpendicular to the coast with increasing water depth ($\leq$80 m). The location of these transects to the northwest of the Santa Clara River mouth was consistent with post-storm and Holocene accumulation of Santa Clara River sediment [*Drake et al.*, 1972; *Dahlen et al.*, 1990]. Surficial grabs and cores of shelf sediment were sampled using a

stainless steel box corer (20 × 30 cm^2). In general, the top portion of the cores (0 to 15 cm) was extruded in 1 cm sections, while the lower portion of each core (15 to 30 cm) was sectioned into 2 cm intervals. Sediments were weighed wet and then dried in 50 °C oven and reweighed to obtain moisture content. Samples were then stored in pre-ashed glass vials until further analysis and quantification of particle-reactive tracers in the laboratory.

3.2. Radionuclide Quantification and Accumulation Rates

[12] Radionuclide analyses were performed following the methodology of *Alexander et al.* [2008]. In brief, dried, ground sediment (~30 g) was gamma-counted for ^{210}Pb (46.5 keV), ^{214}Pb (295 and 352 keV), ^{7}Be (477 keV), ^{214}Bi (609 keV) and ^{137}Cs (661 keV) using a low-background, planar germanium detector (ORTEC LO-AX). Samples were equilibrated for 20 days prior to counting to allow in-growth of ^{222}Rn. Activities of ^{214}Pb and ^{214}Bi were averaged to provide an estimate of ^{226}Ra activity (the effective grandparent of ^{210}Pb). The activities of these nuclides in each sample were calculated in disintegrations per minute per gram of salt-free sediment (dpm g^{-1}), with sample masses corrected for salt content assuming a pore water salinity of 33.4 ‰ (an average bottom water value for the area). Counting errors for total ^{210}Pb, ^{214}Pb and ^{214}Bi were propagated to calculate excess ^{210}Pb (^{210}Pb unsupported by the decay of ^{226}Ra in the seabed; total ^{210}Pb activity minus ^{226}Ra activity) and ranged from 5 to 9 % of the activity, with a mean error of ±8 %, or 0.25 dpm g^{-1}. Vertical accretion and mass flux rates were calculated from the excess ^{210}Pb activity profile data. Mass flux rate was used to calculate depositional fluxes and ages, as these variables account for vertical changes in porosity [*Alexander et al.*, 2008]. Counting errors for ^{137}Cs ranged from 6 to 40 % of the total activity because of extremely low count rates and activities, with a mean error of 21 %, or 0.02 dpm g^{-1}. Sedimentation rates were calculated using the constant rate of supply model [*Appleby and Oldfield*, 1978]. This model assumes a constant rate of supply of excess ^{210}Pb to the sediments that is independent of variations in sedimentation rates.

3.3. Bulk Carbon, Nitrogen, and Stable Isotopes

[13] Bulk OC and nitrogen (N) analyses were performed at University of California-Davis Stable Isotope Laboratory measured on continuous flow Isotope Ratio Mass Spectrometer (Europa Hydra 20/20). In order to remove inorganic carbon from each sample, all sediments were placed in a dessicator for 24 to 48 h with a beaker of 15 mL of concentrated HCl, according to *Harris et al.* [2001]. The average standard deviation of all elemental analyses, determined by replicate analysis of the same sample, was 0.07 ± 0.06 weight %.

3.4. Organic Markers

[14] Sediment organic marker analyses consisted of: PAHs, lignin, and levoglucosan. Dried sediments were extracted and analyzed for PAHs as described by *Arzayus et al.* [2002], modified to utilize microwave assisted solvent extraction. In brief, 3 to 5 g of dried sediment was spiked with a surrogate standard solution containing deuterated PAHs (d_8-naphthalene, d_{10}-anthracene, d_{12}-benzo(a)anthracene, and d_{12}-benzo(a)pyrene). The sample was extracted according to a modified *Bligh and Dyer* [1959] solvent regime with 2:1, v:v CH_2Cl_2/CH_3OH and assisted by microwave energy (ramping up to 115 °C in 8 min and holding for 15 min). The extracts were decanted upon centrifugation for 12 min at 1500 rpm and the process was repeated for a total of 3 extractions. The three sequential extracts for each sample were combined, evaporated, and were then purified by open column solid-liquid chromatography on 100 to 200 μm mesh size silica gel [*Dickhut and Gustafson*, 1995]. Excess sulfur was removed with activated copper granules [*Ozretich and Schroeder*, 1986]. All PAHs were analyzed using a Shimadzu 5050a Series Gas Chromatograph/Mass Spectrometer (GC/MS). The GC/MS was run in selective ion monitoring mode. Recoveries of all PAHs were calculated by comparing yields of deuterated PAHs in a surrogate standard (noted above) to that of deuterated PAHs in an internal standard mixture consisting of d_{10}-acenaphthene, d_{10}- phenanthrene, d_{12}-chrysene, and d_{12}-perylene. The average PAH recoveries across all the samples were: 52.6 ± 11.9; 73.3 ± 7.08; 87.0 ± 11.3; and 74.4 ± 8.37 %, for d_8-naphthalene, d_{10}-anthracene, d_{12}-benzo(a)anthracene, and d_{12}-benzo(a)pyrene, respectively. The response of the GC/MS was quantified by injecting a daily PAH relative response factor standard. For purpose of assessing quality assurance and quality control of PAH extraction, National Institute of Standards and Technology Standard Reference Material (SRM) 1941b (marine sediment) was extracted for PAHs in a manner identical to that used on sediments. The mean recoveries of all certified PAHs in SRM 1941b were 102 ± 41%. Detected quantities of PAHs were deemed reportable if compound masses observed in samples were greater than 3 times that observed in laboratory sand blanks. The 33 PAHs (ranging in molecular weight from 128.17 to 300.35) quantified by these techniques and reported in total PAH values include: naphthalene, 2-methylnaphthelene, azulene, 1-methylnaphthelene, biphenyl, acenaphthylene, acenaphthene, fluorine, 1-methylfluorene, phenanthrene, anthracene, 2-methylphenanthrene, 2-methylanthracene, 1-methylanthracene, 1-methylphenanthrene, 9-methylanthracene, 3, 6-dimethylphenanthrene, fluoranthene, pyrene, 9, 10-dimethylanthracene, retene, benz(a)anthracene, chrysene, benzo(b)fluoranthene, benzo(k)fluoranthene, 7, 12-dimethylbenz(a)anthracene, benzo(e)pyrene, benzo(a)-pyrene, perylene, indeno(1, 2, 3-cd)pyrene, dibenz(a, h)anthracene, benzo(g, h, i)perylene, and coronene.

[15] Levoglucosan was extracted in conjunction with the PAHs [*Simoneit et al.*, 1999; *Elias et al.*, 2001]. A gravimetrically quantified sub-sample of the PAH extract was isolated and derivatized with bis(trimethylsilyl)trifluoroacetamide +1% trimethylchlorosilane (BSTFA) at 70°C for 30 min. Levoglucosan concentrations were then determined using GC/MS selective ion monitoring and quantified against retention time, mass spectral fragmentation according to *Simoneit and Elias* [2001], and an external standard calibration curve of a commercially available high-purity standard. Extraction yields of levoglucosan were not directly measured, but should be analogous to PAH recoveries, as the extraction methods are identical.

[16] Lignin-phenols were extracted according to the method of *Hedges and Ertel* [1982], as modified by *Goni*

and Montgomery [2000] for microwave assisted solvent extraction. For lignin analyses, 1 to 5 g of dried sediment were oxidized under alkaline (2N NaOH) conditions with CuO at 150 °C for 1.5 h in N_2-pressurized Teflon vessels. A recovery standard of ethylvanillin (100 μl of 1 mg mL^{-1} in 1 N NaOH) was added to each vessel immediately following oxidation. After separating the solid residues by centrifugation, the aqueous portion was acidified with concentrated HCl down to a pH of 1 to 2. The CuO oxidation products were separated from the aqueous phase via extraction with ethyl acetate. The extracts were filtered over anhydrous Na_2SO_4 and then blown to dryness under a continuous N_2 stream, or rotary evaporation, and re-dissolved in pyridine. The extracts were stored in a freezer (−20 °C) until analysis by GC/MS. Immediately prior to GC/MS analyses, the CuO oxidation products were derivatized with BSTFA at 70 °C for 30 min and injected into the Shimadzu 5050a Series GC/MS. The response of the GC/MS was linear over a range of concentrations for individual phenols in a mixed standard. Thus a two-point calibration curve using a specific concentration of the mixed standard was used on a daily basis to confirm retention times, mass spectra, and response factors for each target phenol. Using this procedure, the OC-normalized yields of eight lignin-derived reaction products, including vanillyl (V) phenols (vanillin, acetovanillone, vanillic acid), syringyl (S) phenols (syringealdehyde, acetosyringone, syringic acid), and cinnamyl (C) phenols (*p*-coumaric acid, ferulic acid) were estimated [*Hedges and Mann*, 1979]. Lignin-phenol concentrations are presented using the lambda indices as typical for estimating the relative contribution of lignin-phenols to total OC in sediments.

4. Results

4.1. Sediment Deposition and Accumulation

[17] The ^{7}Be surficial activities ranged from 0.07 to 1.13 dpm g^{-1} (Table 1). The highest ^{7}Be activity was observed at Station 15, whereas moderate levels of ^{7}Be were noted at Stations 21, 22, and 24. The spatial distribution of flood-derived sediment as indicated by ^{7}Be [e.g., *Sommerfield et al.*, 1999] was focused near Stations 15 and 24. Profiles of radiogenic isotopes used to quantify sediment deposition are shown in Figure 3. Both the x-radiograph and ^{210}Pb activity showed a surface mixed layer from 0 to ~4 cm in depth, and a low density, low ^{210}Pb activity layer which occurred in the surface (Figure 3). This appears to correspond with the most recent flood layer of the 2004 winter, as high water content and low ^{210}Pb activity is indicative of California shelf flood sediments [e.g., *Leithold and Hope*, 1999; *Sommerfield and Nittrouer*, 1999; *Blair et al.*, 2004; *Leithold et al.*, 2005].

[18] The relatively steep slope of the excess ^{210}Pb decay profile for Station 24 indicates rapid accumulation, although the x-radiograph suggests some biological mixing may have influenced the profile (Figure 3). The activity of excess ^{210}Pb decays exponentially from 5 to 21 cm, followed by a zone of low excess activity sediment from 21 to 25 cm depth and a return to higher excess activities from 25 to 30 cm (the bottom of the core). The low excess activity layer at 21 to 25 cm has the ^{210}Pb radiochemical characteristics of a flood deposit. If so, this layer would have been rapidly emplaced. Unfortunately, the x-radiograph depicts only the upper 17 cm of the core, so visual documentation of this deeper layer is not available to provide further evidence of this layer's structure. The vertical accretion rate of the 5 to 21 cm portion of the core was calculated to be 0.99 cm a^{-1}. This value is not corrected for changes in porosity down core, thus we also report a mass flux rate of 1.35 g cm^{-2} a^{-1}, which inherently corrects for these changes. We assessed ^{137}Cs chronology in an attempt to validate the ^{210}Pb results, but a distinct peak, indicative of the year 1963, was not evident in the ^{137}Cs profile (Figure 3). Accumulation rates at the remaining sites ranged from 0.49 to 0.88 cm a^{-1} in magnitude and showed similar subsurface features [*Alexander et al.*, 2008].

4.2. Spatial Distributions of Carbon and Chemical Markers in Surface Sediments

[19] Bulk OC abundance and isotopic signatures for surface sediments are noted in Table 1 and depicted in Figure 4. The overall range in OC across the surface sediment stations was 0.10 to 2.2 %. Stations 3 and 24 showed an anomalous depletion of $\delta^{13}C_{OC}$ values, while station 21 was enriched in $\delta^{13}C_{OC}$ (both greater than ±1 std. dev) (Figure 4). The average surficial $\delta^{13}C_{OC}$ value of −23.3 ± 0.7 ‰ for all stations closely matched the average $\delta^{13}C_{OC}$ values of −22.2 ± 0.8 ‰ for Santa Clara particulate OC as observed by *Masiello and Druffel* [2001]. Further, elevated atomic carbon to nitrogen ratios (OC:N) occurred at/near Stations 3 and 24 (Figure 5). Although these bed sediment OC:N ratios were not as high as typically known to occur in coastal systems dominated by terrigenous organic matter influx [e.g., *Goni et al.*, 1997; *Onstad et al.*, 2000; *Gordon and Goni*, 2004], our sedimentary OC:N values were not significantly different ($p < 0.05$) from *Masiello and Druffel* [2001] for Santa Clara river suspended particulates (discharge weighted mean OC:N of 11.2 ± 0.08).

[20] Abundances of organic markers in surface sediments are also shown in Table 1. The concentrations of tPAHs in Santa Barbara Channel sediments ranged from 201.7 to 1232.3 ng gdw^{-1} (mean = 782.0 ± 360.6 ng gdw^{-1}). Station 24 had the highest concentration of tPAHs, however nearby stations 3 and 23 also showed considerable levels at 1073.5 and 1120 ng gdw^{-1}, respectively. Relative to the PAH molecules quantified, phenanthrene and perylene occurred at elevated concentrations in surface sediments (Table 1). Phenanthrene exhibited the highest overall abundance, 411.4 ng gdw^{-1} or 36.7% of tPAHs, with an average concentration of 165.9 ± 128.8 ng gdw^{-1}. In these samples, parent PAHs were found in greater abundance versus alkylated homologues, with ratios of 2.96 ± 1.69 (Table 1). Perylene was found in the Santa Barbara Channel surface sediments ranging from 15.1 to 386.0 ng gdw^{-1}. Another PAH of interest, retene (3-ring), was also found in the Santa Barbara surface sediments between 0.64 and 2.67 ng gdw^{-1}. The highest concentrations of retene were found in surface sediments at stations 15, 20 and 24.

[21] Spatial distribution of levoglucosan and lignin phenols generally corroborate the trends in PAH distributions (Figure 5), with elevated levels near Stations 3 and/or 24. Levoglucosan concentrations in surficial sediments ranged from 1.26 to 6.92 μg gdw^{-1}. Lignin (λ_6) abundance in

Table 1. Areal Distribution of Radionuclides, Supplemental Geochemical Markers, and Selected PAHs in Surface Sediments of the Santa Barbara Channel[a]

Station ID	1	2	3	15	18	20	21	22	23	24
Geospatial Parameters										
Longitude, deg	119.40	119.41	119.45	119.43	119.37	119.50	119.53	119.49	119.46	119.43
Latitude, deg	34.31	34.30	34.27	34.28	34.23	34.30	34.35	34.33	34.31	34.26
Water depth, m	20	30	50	40	25	57	40	40	40	40
Radionuclides, dpm g^{-1}										
^{7}Be	0.28 (0.08)	0.21 (0.1)	0.24 (0.1)	1.13 (0.15)	0.07 (0.06)	0.28 (0.09)	0.48 (0.12)	0.44 (0.1)	0.22 (0.09)	0.41 (0.11)
^{137}Cs	0.08 (0.02)	0.26 (0.03)	0.23 (0.03)	0.15 (0.03)	0.03 (0.01)	0.36 (0.03)	0.19 (0.03)	0.33 (0.04)	0.25 (0.02)	0.16 (0.02)
$^{210}Pb_{exs}$	0.62 (0.18)	6.01 (0.3)	5.45 (0.32)	5.85 (0.35)	0.83 (0.14)	14.32 (0.26)	7.78 (0.35)	7.38 (0.35)	7.66 (0.22)	1.84 (0.18)
Supporting Geochemistry										
Water content, %	9.56 (0.02)	35.57 (0.07)	53.66 (0.05)	48.03 (0.03)	11.48 (0.02)	46.24 (0.09)	43.63 (0.06)	47.14 (0.12)	42.46 (0.04)	38.07 (0.04)
Organic carbon, %	0.24 (0.02)	0.82 (0.02)	2.18 (0.02)	0.96 (0.002)	0.10 (0.01)	1.28 (0.005)	1.18 (0.003)	1.17 (0.01)	1.05 (0.01)	1.14 (0.03)
Carbon/Nitrogen (C:N)	8.74 (0.60)	9.63 (0.04)	13.39 (0.11)	10.03 (0.03)	5.75 (0.20)	10.15 (0.01)	9.99 (0.04)	10.02 (0.02)	9.89 (0.07)	12.80 (0.31)
$\delta^{13}C$, ‰	−22.94 (0.15)	−22.79 (0.002)	−24.56 (0.05)	−23.20 (0.02)	−23.65 (0.03)	−22.96 (0.001)	−22.55 (0.002)	−22.73 (0.01)	−22.86 (0.03)	−24.45 (0.04)
$\lambda 6$ lignin (mg per 100 mg OC)	0.41 (0.04)	0.64 (0.06)	1.07 (0.09)	0.70 (0.06)	0.34 (0.03)	NS ()	0.61 (0.05)	0.54 (0.05)	0.63 (0.06)	2.16 (0.19)
Levoglucosan, $\mu g\ g^{-1}$	2.08 (0.17)	3.92 (0.32)	6.92 (0.57)	6.35 (0.52)	2.18 (0.18)	2.97 (0.24)	6.47 (0.53)	5.63 (0.46)	2.31 (0.19)	1.26 (0.10)
PAHs, ng g^{-1}										
Acenaphthylene	2.43 (0.09)	4.92 (0.18)	140 (0.05)	2.51 (0.09)	7.14 (0.27)	8.57 (0.32)	4.92 (0.18)	10.15 (0.38)	2.44 (0.09)	2.88 (0.11)
Acenaphthene	9.45(0.28)	15.84 (0.47)	9.91 (0.29)	11.16 (0.33)	11.97 (0.36)	29.80 (0.88)	46.90 (1.39)	17.68 (0.52)	48.77 (1.45)	9.73 (0.29)
Fluorene	3.81 (0.41)	5.98 (0.64)	9.93 (1.06)	3.46 (0.37)	5.24 (0.56)	10.18 (1.09)	16.14 (1.73)	16.74 (1.79)	21.54 (2.31)	5.25 (0.56)
Phenanthrene	64.83 (5.22)	96.95 (7.81)	97.78 (7.88)	112.19 (9.04)	50.28 (4.05)	138.03 (11.12)	388.08 (31.27)	113.73 (9.17)	411.37 (33.15)	186.10 (15.00)
Anthracene	0.62 (0.05)	0.58 (0.05)	1.92 (0.16)	1.03 (0.09)	0.54 (0.05)	1.11 (0.10)	0.70 (0.06)	0.55 (0.05)	1.29 (0.11)	2.27 (0.20)
Fluoranthene	7.88 (0.36)	9.45 (0.44)	21.27 (0.98)	13.57 (0.63)	1.74 (0.08)	15.44 (0.71)	13.69 (0.63)	12.90 (0.60)	13.41 (0.62)	109.17 (5.04)
Pyrene	6.70 (0.26)	14.78 (0.56)	28.60 (1.09)	22.12 (0.84)	4.00 (0.15)	21.96 (0.84)	21.33 (0.81)	18.12 (0.69)	18.30 (0.70)	117.25 (4.47)
Retene	0.64 (0.05)	1.13 (0.08)	2.35 (0.17)	2.67 (0.20)	1.01 (0.07)	2.63 (0.19)	2.24 (0.17)	2.39 (0.18)	1.74 (0.13)	2.43 (0.18)
Benz[a]anthracene	2.56 (0.02)	4.76 (0.03)	11.07 (0.08)	6.78 (0.05)	1.64 (0.01)	7.41 (0.05)	6.82 (0.05)	8.81 (0.06)	6.35 (0.04)	10.83 (0.08)
Chrysene	7.92 (0.28)	20.25 (0.72)	37.22 (1.32)	22.99 (0.81)	4.23 (0.15)	29.28 (1.04)	20.62 (0.73)	24.04 (0.85)	21.07 (0.75)	82.78 (2.93)
Benzo[b]fluoranthene	3.80 (0.09)	10.14 (0.23)	22.76 (0.51)	12.36 (0.28)	1.56 (0.04)	14.60 (0.33)	14.60 (0.33)	11.12 (0.25)	13.81 (0.31)	35.04 (0.79)
Benzo[k]fluoranthene	1.77 (0.04)	12.29 (0.28)	34.13 (0.77)	17.01 (0.38)	1.64 (0.04)	20.05 (0.45)	10.38 (0.23)	16.26 (0.37)	18.07 (0.41)	96.56 (2.17)
Benzo[e]pyrene	3.21 (0.09)	7.74 (0.22)	18.24 (0.52)	10.03 (0.29)	2.39 (0.07)	11.04 (0.31)	11.36 (0.32)	9.76 (0.28)	10.38 (0.30)	19.15 (0.55)
Benzo[a]pyrene	9.37 (0.25)	18.24 (0.48)	27.38 (0.72)	19.96 (0.53)	3.50 (0.09)	20.50 (0.54)	16.83 (0.44)	16.12 (0.43)	21.08 (0.56)	27.35 (0.72)
Perylene	46.08 (1.63)	145.58 (5.13)	385.96 (13.61)	223.88 (7.90)	15.11 (0.53)	208.17 (7.34)	191.56 (6.76)	164.05 (5.79)	196.76 (6.94)	207.52 (7.32)
Indeno[1, 2, 3-cd] pyrene	4.16 (0.08)	12.02 (0.24)	25.52 (0.51)	14.99 (0.30)	1.31 (0.03)	15.82 (0.32)	12.51 (0.25)	13.23 (0.27)	10.36 (0.21)	38.37 (0.77)
Benzo[g, h, i]perylene	4.40 (0.08)	22.77 (0.40)	40.11 (0.71)	25.35 (0.45)	1.30 (0.02)	30.51 (0.54)	27.12 (0.48)	23.92 (0.43)	23.40 (0.42)	40.99 (0.73)
Parent/Alkyl Ratio	4.31 (0.90)	2.3 (0.48)	1.04 (0.22)	1.75 (0.37)	2.84 (0.60)	1.82 (0.38)	5.74 (1.20)	1.93 (0.40)	5.69 (1.19)	2.20 (0.46)
Total PAHs	245.5 (11.9)	568.7 (27.7)	1073.6 (52.2)	726.4 (35.3)	201.7 (9.8)	851.2 (41.4)	1076.9 (52.4)	723.6 (35.2)	1120.0 (54.5)	1232.3 (59.9)

[a]NS = insufficient sample mass or sample not analyzed. Uncertainty in parentheses for radionuclides is explained in the text. For geochemical variables, values in parentheses are the standard error about the mean of duplicate analyses from the same depth interval in one core. For PAHs, values in parentheses are the standard deviation of analytical measurement error propagated through the entire extraction and analytical procedure.

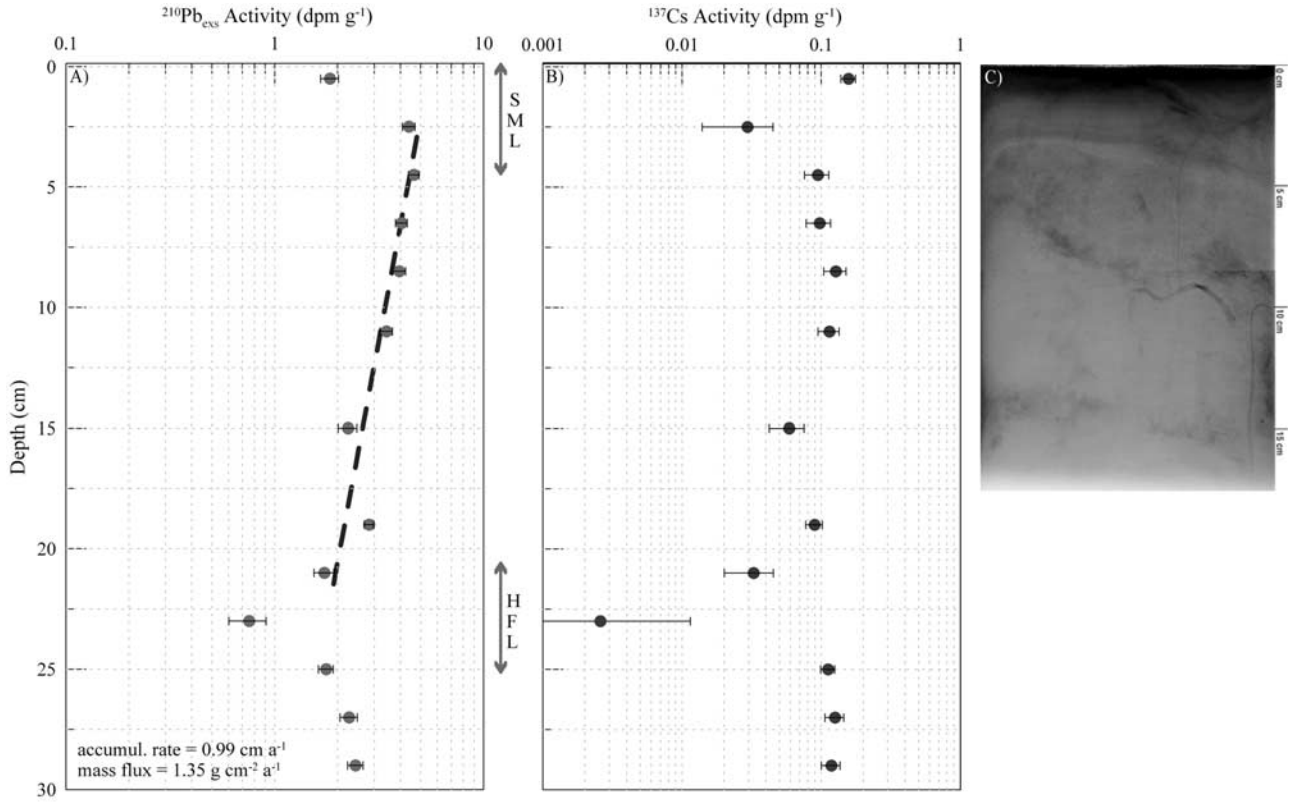

Figure 3. Profiles of (a) Excess ^{210}Pb activity, (b) ^{137}Cs activity, and (c) X-radiograph at Station 24. Average sedimentation and mass accumulation rates ($r^2 = 0.84$, $p < 0.05$) are derived from regression of 5 to 21 cm interval, as activity in this region exhibited sufficient total and background activity with steady state radioactive decay. Note the surface mixed layer (SML) from ~0 to 4 cm, and historic flood layer (HFL) from ~21 to 25 cm.

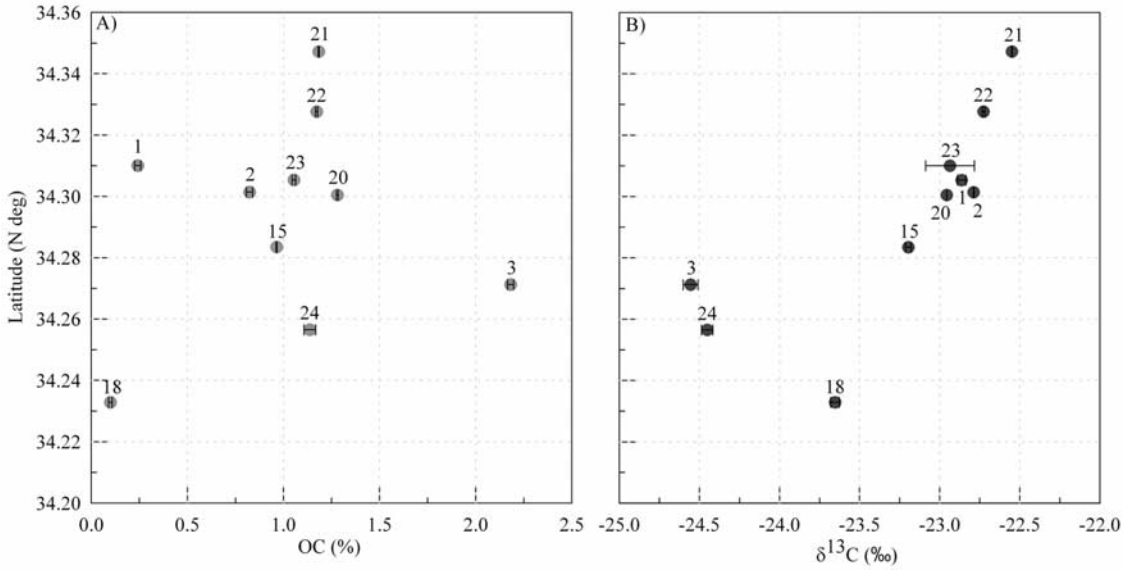

Figure 4. Spatial distribution of (a) Organic Carbon (OC), and (b) $\delta^{13}C_{OC}$ (‰) for surface sediments delivered to the Santa Barbara Channel following 2003 wildfires. Number near datapoint denotes Station ID from Figure 1. Latitude serves as a proxy for distance from river mouth, however is not precise due to depositional setting and transect orientation (refer to Figure 1). Magnitude $\delta^{13}C_{OC}$ (‰) in relation to PDB standard.

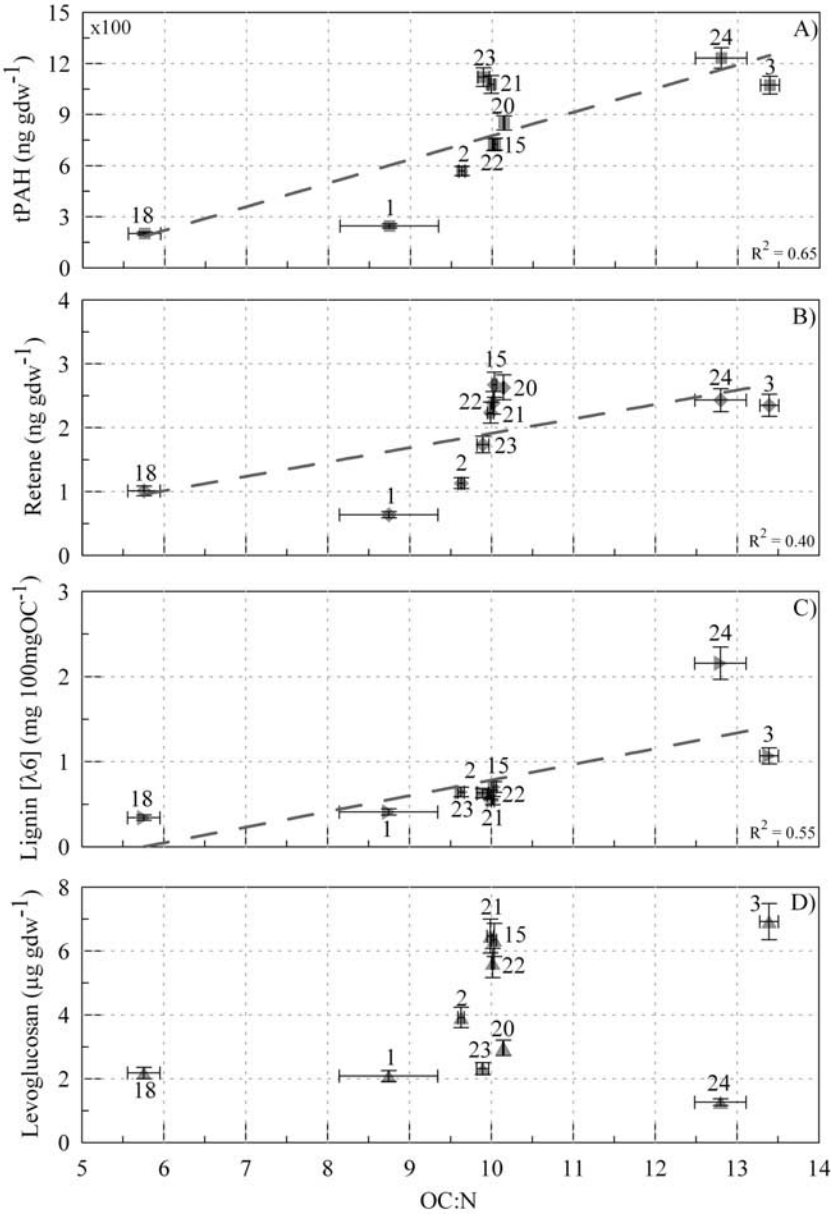

Figure 5. Relationship between (a) total polycyclic aromatic hydrocarbons (tPAH), (b) retene, (c) lignin phenols, and (d) levoglucosan and organic carbon to nitrogen ratio (OC:N) for surficial sediments. Diagonal line represents significant linear regressions ($p < 0.05$) between the dependant and independent variable in each graph. The regression between levoglucosan and OC:N was not significant. Numbers denote station id.

surficial sediments ranged from 0.3 to 2.2 mg per 100 mg of the sedimentary OC (Figure 5).

4.3. Down Core Profiles of Carbon and Chemical Markers

[22] The spatial trends noted above suggest that initial deposition and/or redistributed settling of terrestrial burn-derived material occurred near stations 3 and 24, and at 40 to 50 m water depth, which generally agrees with previous work [*Drake et al.*, 1972; *Thorton*, 1984]. A large interval of sediment from deeper in the core collected at Station 3 was lost during sample handling. Thus, down core chemical marker analysis was conducted specifically at Station 24. The down core profiles of OC abundance, its stable isotopic signature, and organic markers for Station 24 are shown in Figure 6.

[23] The down core average of OC, OC:N ratio, and $\delta^{13}C_{OC}$ was 0.61 ± 0.16 %, 10.34 ± 1.2, and −24.1 ± 0.34 ‰, respectively. The abundance of OC and OC:N molar ratios exhibited >1 standard deviation difference from the down core average at two locations in the core: the surface and at ~22 cm depth (Figure 6). Similarly, values of $\delta^{13}C_{OC}$ show 1 to 2 ‰ depletion at the surface and at 20 to 22 cm depth.

[24] Levoglucosan abundance averaged 1.2 ± 1.2 μg gdw^{-1} throughout the core. Elevated concentrations of levoglucosan were observed at 3 cm depth (2.3 μg gdw^{-1})

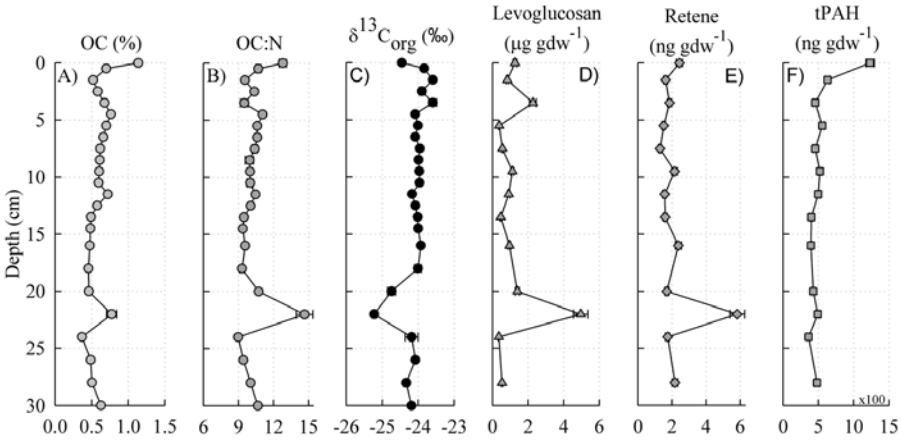

Figure 6. Geochemical profiles of (a) percent organic carbon (%OC), (b) organic carbon to nitrogen ratio (OC:N), (c) stable carbon isotope ($\delta^{13}C_{OC}$), (d) levoglucosan, (e) retene, and (f) total PAHs. Note deviations from background near the surface 0 to 4 cm and at the depth interval 21 to 25 cm, apparently due to massive wildfire-derived inputs.

and again at 22 cm depth (4.9 μg gdw^{-1}). Retene concentrations ranged from 1.3 to 5.8 ng gdw^{-1}. The greatest retene abundance was observed at the 22 cm depth, which surpassed the surface (0 to 3 cm) retene average of 1.92 ± 0.71 ng gdw^{-1}. The down core tPAH concentrations ranged from 359.9 to 1232.3 ng gdw^{-1}, with surficial sediments exhibiting the greatest abundance. Down core lignin profiles (not shown) exhibited a directly proportional relationship with levoglucosan ($r^2 = 0.66$, $p < 0.05$) and retene ($r^2 = 0.84$, $p < 0.05$) from 0 to 30 cm depth. Overall, OC, OC:N ratio, $\delta^{13}C_{OC}$, levoglucosan, retene, and lignin phenols follow parallel profiles as tPAHs in the surface and near the 22 cm sediment layer (Figure 6).

5. Discussion

[25] The drainage basin of the Santa Clara River yields 1500 to 3600 t km^{-2} yr^{-1} of sediment from the Western Transverse Range directly into the Santa Barbara Channel [*Scott and Williams*, 1978; *Inman and Jenkins*, 1999; *Warrick*, 2002]. Further, the Santa Clara may serve as a model for small mountainous watersheds delivering high loads of refractory organic matter and nutrients directly to the coastal ocean [e.g., *Masiello and Druffel*, 2001; *Komada et al.*, 2004; *Warrick et al.*, 2005].

[26] According to our study, concentrations of PAHs in surface sediments are indicative of substantial hydrocarbon inputs. Phenanthrene levels at ~36.7 % of total PAHs in our samples are consistent with other combustion product analyses of plant materials [e.g., *Ramdahl et al.*, 1982; *McGrath et al.*, 2001; *Schauer et al.*, 2001]. Perylene and retene levels were also elevated, suggesting influxes due to either pyrogenic or petrogenetic processes. Although perylene can result from non-pyrolytic processes [*Silliman et al.*, 2001; *Countway et al.*, 2003], retene is primarily considered a molecular marker of wood combustion [*Ramdahl*, 1983], though possibly formed during early diagenesis from dehydrogenation of abietic acid from woody debris [*Laflamme and Hites*, 1978]. We interpret the elevated concentrations of retene in these sediments to be indicative of the presence of combusted woody-debris, as noted in other post-wildfire studies of soil geochemistry [*Oros et al.*, 2002; *Otto et al.*, 2006].

[27] We discount the notion that petroleum seeps contribute to the PAH levels in these samples for the following reason. Unsubstituted PAHs typically dominate over their alkylated homologs when derived from pyrolysis [*Killops and Massoud*, 1992; *Jiang et al.*, 1998]. Alternatively, alkylated PAHs exceed their parent homologs when uncombusted petroleum is a potential source of PAHs [*Blumer and Youngblood*, 1975]. Since burning tends to create PAH mixtures dominated by unsubstituted PAHs [*Jiang et al.*, 1998], the high parent to alkyl ratios (2.96 ± 1.69) are suggestive of pyrolysis as the predominant source of PAHs at our sites.

[28] Lignin comprises the cell walls of vascular plants, and lignin oxidation products can be isolated in coastal sediments [*Hedges and Mann*, 1979]. Lignin phenols have been used to quantify the magnitude of terrestrial organic material delivered to the sedimentary environment [e.g., *Hedges and Mann*, 1979; *Goni et al.*, 1997]. Similarly, levoglucosan has been determined to be a unique cellulose carbohydrate by-product of biomass combustion [*Simoneit et al.*, 1999], thus providing information about wildfire-derived input to a system [*Elias et al.*, 2001]. The correlated abundances of $\delta^{13}C_{OC}$, PAHs, retene, levoglucosan, and lignin in our study establish that wildfires may be important in the transport of lignin and pyrolyzed carbonaceous compounds from the Santa Clara watershed into the Santa Barbara Channel (e.g., Figures 4 to 6). Taken together, these chemical markers provide corroborating evidence that extensive pyrolyzed and biomass-derived material was transported to the Santa Barbara Channel during the 2004 winter storms. Indeed, as discussed below, we posit that the combination of these geochemical tracers can provide accurate evidence for historic wildfires in the sedimentary record.

[29] The 1985 fires in the Santa Clara River watershed were the 5th largest on record (1910 to 2006; Figure 2) in terms of watershed area burned (275.8 km^2; CaDFFP http://

frap.cdf.ca.gov/data/) and would represent the 2nd largest area burned during the timespan captured in our geochemical profile (~1970 to early 2004). Using the depth-averaged accumulation rate (0.99 cm a^{-1} or 1.35 g cm^{-2} a^{-1}) obtained from the 5 to 21 cm interval, the 21 to 25 cm depth interval in our sediment core at Station 24 corresponds to ~1985 (±1.2 years). Thus, we suspect that the flood layer indicated by the trend in ^{210}Pb activity in the depth interval 21 to 25 cm of this core is associated with enhanced deposition following the 1985 fire event.

[30] The ratio of OC:N, $\delta^{13}C_{OC}$, levoglucosan, and lignin phenols also follow parallel profiles as PAHs in the deeper sediment layers Figure 6. Indeed, down core tPAHs in the Santa Barbara Channel are well correlated ($r^2 \geq 0.66$, $p < 0.05$) with OC:N, lignin, and levoglucosan. Similar to our record of $\delta^{13}C_{OC}$ in surface sediments and those across the 21 to 25 cm depth interval, *Schimmelmann and Tegner* [1991] found that years of high terrestrial input generally showed an average depletion of up to 2 ‰ in the central Santa Barbara basin. As noted above, retene concentration of 5.82 ng gdw^{-1} was observed at a depth of 22 cm, exceeding the surface sediment (0 to 3 cm) retene value of 1.92 ± 0.71 ng gdw^{-1}. Levoglucosan abundance generally follows other marker profiles with depth (Figure 6), although the upper (0 to 2 cm) peak expected for the 2003 fires was found below the surface mixing layer. Furthermore, there was a levoglucosan peak at the subsurface layer at 21 to 25 cm depth corresponding to same depth interval where notable shifts occurred in other organic tracers (Figure 6).

[31] Our results suggest that the Santa Clara River is an important contributor of fire-derived carbon compounds to the Santa Barbara Channel and possibly to the open ocean. In order to place our results into a global context, we compared oceanic loading of tPAHs delivered from the Santa Clara into the Santa Barbara Channel to other coastal shelf systems (non-enclosed, direct dispersal) globally to highlight the importance of oceanic loading of wildfire-derived compounds.

[32] The Santa Clara delivers >50 % of its annual sediment load (~3.5Mt) in less than 2 % of the year on average [*Warrick*, 2002; *Warrick et al.*, 2004]. The rapid and massive dispersal of sediment by the Santa Clara apparently delivered abundances of 201.7 to 1232.3 ng gdw^{-1}, 0.64 to 2.67 ng gdw^{-1}, 0.3 to 2.2 mg per 100 mg OC, and 1.3 to 6.9 μg gdw^{-1} for total PAHs, retene, lignin, and levoglucosan, respectively, following the 2003 wildfires. On the basis of average surface and down core concentrations, the average annual flux of tPAHs, levoglucosan, and lignin, respectively, to the Santa Barbara Channel was calculated to be 885.5 ± 170.2 ng cm^{-2} a^{-1}, 3.5 ± 1.9 μg cm^{-2} a^{-1} and 1.4 ± 0.3 mg per 100 mg OC cm^{-2} a^{-1} over ~30 years. A conservative estimate suggests that the 2003 wildfires resulted in a yield of ~1725.2 g km^{-2} a^{-1} of PAHs from the Santa Clara watershed directly into the Santa Barbara Channel. Over the depositional timeframe covered in our work (~30 a), the average accumulation of fire-derived PAHs at station 24 was 715.3 ± 222.8 ng cm^{-2} a^{-1}, although certain events (i.e., 1985, 2003) may exceed these levels by orders of magnitude.

[33] The sedimentary yields of tPAHs imparted to continental margin sediments and delivered to the Santa Barbara Channel after the 2003 wildfires (and subsequent 2004 floods) rival and exceed numerous other coastal settings for which tPAH data exist (Figure 7). The concentrations of tPAHs in Santa Barbara Channel sediments ranged from 201.7 to 1232.3 ng gdw^{-1} (mean = 782.0 ± 360.6) (Table 1). From this, we calculate that the Santa Clara tPAH yield conservatively ranges from 282.4 to 1725.2 g km^{-2} a^{-1}, utilizing sediment yield values reported in *Milliman and Syvitski* [1992]. The other coastal settings were chosen based on their limited residence time and close hydraulic connection with the ocean (i.e., non-enclosed, direct dispersal). Of the 21 other coastal settings reviewed, only one (Gao Ping River-coast) exhibited higher tPAH yield than those observed in the Santa Barbara Channel (Figure 7). In addition to those settings featured in Figure 7, we considered tPAH yield in coastal sediments from upland and lowland river discharge sites [*Milliman and Syvitski*, 1992]; however these systems were not included in Figure 7 for two reasons: 1) these systems typically drained highly perturbed (e.g., dams, industry, anthropogenic point source contamination) landscapes, and 2) tPAH yields were typically 2+ orders of magnitude lower than the Santa Clara.

[34] What is striking about the PAH levels in the Santa Barbara Channel is that the prevailing wind patterns in Southern California are to the East [e.g., *Dorman and Winant*, 2000], minimizing the role of atmospheric deposition in PAH loading to this coastal system. We cannot discount the fact that high velocity offshore winds such as the Santa Ana winds [*Miller and Schlegel*, 2006] may deposit fire-derived material into the ocean, which may then settle into bed sediments. However, we did not observe char or soot layers in the sediment profile; any elevated pyrolysis markers were associated with sediments, suggesting that most of the biomarker distributions we quantified are fluvial in origin. The other coastal systems in Figure 7 are influenced by PAH loading from both atmospheric deposition and fluvial discharge. Additionally, the Gao Ping watershed is suggested to be one of the most anthropogenically perturbed watersheds in Taiwan [*Doong and Lin*, 2004]. Our data indicate that the Santa Clara watershed is an end-member in which biomass combustion by wildfires, followed by erosion and fluvial discharge, may introduce substantial amounts of PAHs directly into the Santa Barbara Channel.

[35] Our methods and other historical information suggest that watersheds draining into the Santa Barbara Channel impart a wildfire signature on bed sediments regularly, as this area is highly susceptible to fire (Figure 2). Wildfires of the Santa Clara watershed are recorded in both recent and relict sediments of the Santa Barbara Channel. For instance, *Mensing et al.* [1999] analyzed charcoal abundance in a deeper Santa Barbara basin core confirming the regular occurrence of wildfire-derived charcoal in the sedimentary record. Although their period of study did not overlap with ours and allow a direct comparison between methods, our multiple chemical marker approach does demonstrate that there are non-charcoal based methods to finding evidence of historical fires in the sedimentary record. Finally, if the frequency of fires and abundance of sediment yield of the Santa Clara are both representative of other SMRs globally, then, as a class of rivers, SMRs may contribute substantial

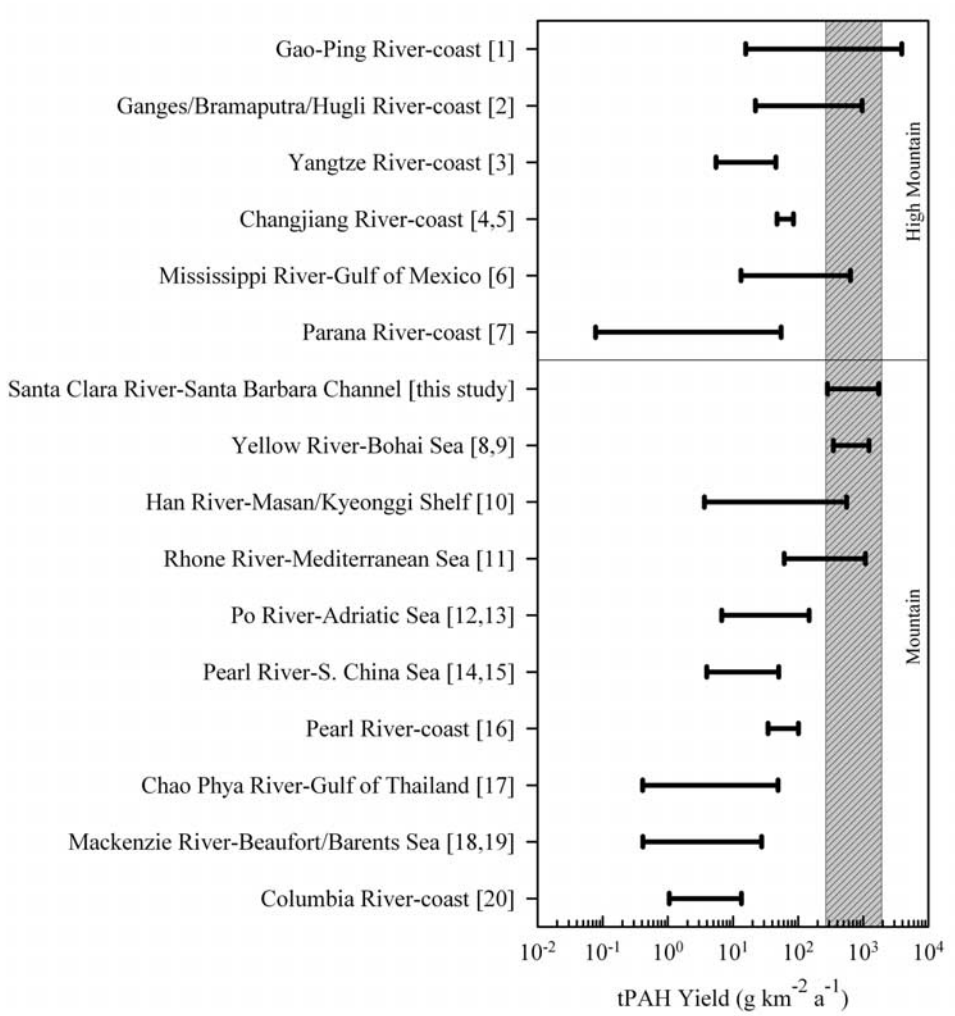

Figure 7. Comparison of total PAHs yield for coastal settings with river particulate dispersal directly to coastal shelf sediments. Shadow highlights the excessive level of post-wildfire tPAHs deposited in Santa Barbara Channel. River sediment yield (t km^{-2} a^{-1}) from *Milliman and Syvitski* [1992] for the dominate dispersal system was multiplied by surficial tPAHs concentration (ng gdw^{-1}) at each locale to calculate tPAH yield. Watershed classification (right) adapted from *Milliman and Syvitski* [1992]. Sediment tPAHs sources: [1-*Doong and Lin*, 2004], [2-*Guzzella et al.*, 2005], [3-*Bouloubassi et al.*, 2001], [4-*Li*, 2000; 5-*Qiu et al.*, 1991], [6-*Overton et al.*, 2004], [7-*Colombo et al.*, 2006], [8-*Bigot et al.*, 1989; 9-*Li*, 2000], [10-*Kim et al.*, 1999], [11-*Lipiatou and Saliot*, 1991], [12-*Magi et al.*, 2002; 13-*Guzzella and DePaolis*, 1994], [14-*Yang*, 2000; 15-*Chen et al.*, 2006], [16-*Luo et al.*, 2006], [17-*Boonyatumanond et al.*, 2006], [18,19-*Yunker et al.*, 1996, 2002], [20-*Prahl and Carpenter*, 1983].

terrestrial and pyrolyzed refractory organic matter to coastal sediments and eventually, the ocean.

6. Conclusions and Implications

[36] Geochemical research on contemporary sediments and soils has shown that fires result in excessive atmospheric and soil loading of organic compounds such as isoprenoids, unsaturated hydrocarbons, refractory charcoal, and black carbon [e.g., *Oros et al.*, 2002; *Simoneit*, 2002; *Lynch et al.*, 2004; *Otto et al.*, 2006; *Rumpel et al.*, 2006]. Furthermore, pyrolysis sequesters carbon from the labile compartment to the refractory compartment [*Shafizadeh*, 1982; *Evans and Milne*, 1987; *McGrath et al.*, 2001; *Lynch et al.*, 2004]. Subsequent dispersal of wildfire residues may have profound impacts on sequestration of carbon as this refractory material is not easily oxidized or degraded [*Gonzalez-Perez et al.*, 2004] and it may be preferentially eroded from the landscape [e.g., *Garcia-Falcon et al.*, 2006]. With time, the amount of wildfire carbonaceous residue in soils tends to decrease as a consequence of erosion [e.g., *Oros et al.*, 2002; *Kim et al.*, 2003; *Garcia-Falcon et al.*, 2006; *Olivella et al.*, 2006]. While data sets for delivery of terrestrial organic matter to coastal environments do exist [e.g., *Hedges and Mann*, 1979; *Goni et al.*, 1997; *Mitra et al.*, 2000; *Onstad et al.*, 2000; *Gordon and Goni*, 2004], we are aware of only one study quantifying sedimentary lignin and PAHs [*Prahl and Carpenter*, 1983], a study for which the focus was the

association between the two classes of molecules. Our study used biomarkers (PAH, lignin, and levoglucosan), as well as molar ratios and carbon isotope signatures in a multitracer approach to quantify the role of wildfire and erosion on coastal deposition of pyrolyzed organic matter. The results of our study indicate that wildfire disturbances near coastal watersheds can be important in the transport of terrestrial and pyrolyzed refractory carbonaceous compounds to the ocean.

[37] Assessing the oceanic discharge of wildfire-derived carbonaceous compounds is relevant to understanding the relative roles of land perturbations on the ocean's carbon cycle in recent times and historically. Over geologic time, the concentrations of atmospheric CO_2 and CH_4, the primary drivers of global climate change, are regulated by transfers of OC between the bio-hydro-atmosphere and the geosphere. The great majority of OC is labile and rapidly cycles between these carbon reservoirs, while a small fraction remains inert, or becomes inert, and is preserved over geological time. Creation and transfer of refractory carbon to the geosphere, i.e., 'carbon sequestration', is one of the keys to understanding current and ancient atmospheric oxygen and CO_2 cycles [*Berner*, 1982]. Exactly how this OC is transferred from labile to refractory pools, and hence, is sequestered, is unclear. If historical combustion processes result in creation of appreciable amounts of refractory carbon, then quantifying erosion and introduction of pyrolyzed carbon into coastal sediments may be an important step to accurately refining estimates of coastal carbon burial and how burial of such wildfire-derived compounds affects global carbon budgets.

[38] Globally, continental margins (shelf, slope and rise) are the most significant reservoirs of marine OC [*Berner*, 1982]. Although margins make up ~15% of the ocean floor, 25 to 50 % of the world's primary production occurs in coastal regions [*Wollast*, 1998; *Walsh*, 1991]. Terrestrial OC delivered by rivers will also mainly be deposited there. As a result, it is estimated that continental margin sediments (including deltas) are responsible for about 80 to 90 % of the ocean's sedimentary OC reservoir [*Berner*, 1982; *Hedges and Keil*, 1995]. Despite efforts to understand the short and long term cycling of carbon derived from both natural and anthropogenic sources, the role of the coastal zone in sequestering carbon is still uncertain [*Sigman and Boyle*, 2000; *NAS*, 2001; *Sarmiento and Gruber*, 2002]. Given the sediment and chemical yields for the Santa Clara, other small mountainous rivers in erosive settings may also yield excessively high levels of pyrogenic PAHs to the coastal ocean following wildfires. In light of recent findings demonstrating substantial refractory carbon export by small mountainous rivers globally [e.g., *Komada et al.*, 2004, 2005; *Carey et al.*, 2005; *Kao et al.*, 2006; *Leithold et al.*, 2006], additional oceanic loading of pyrolyzed compounds, as quantified in this study, may substantially affect coastal carbon budgets.

[39] **Acknowledgments.** The authors thank the Associate Editor and two anonymous reviewers for their time and valuable comments. Funding for GBH was provided by the USEPA GRO Fellowship (#MA-91637001-1). Funding to conduct the extractions and analyses was provided to SM by the NSF–BES and the ACS–Petroleum Research Fund. Funding for vessel time and sample collection was provided by the USGS Coastal and Marine Geology Program. We thank California Department of Forestry and Fire Protection for web access to geospatial wildfire data. The views expressed herein are those of the authors' and do not represent, either expressed or implied, the official policies, regulations, or otherwise of U.S. government agencies or affiliates.

References

Alexander, C., et al. (2008), Sediment accumulation on the shelf and upper slope of the Southern California Margin during the 20th Century, in *GSA Special Publication: Earth science in the urban ocean: The southern California Continental Borderland*, edited by H. Lee et al., in press.

Almendros, G., et al. (1990), Fire-induced transformation of soil organic matter from an oak forest - An experimental approach to the effects of fire on humic substances, *Soil Sci.*, *149*, 158–168.

Andrews, E. D., et al. (2004), Influence of ENSO on flood frequency along the California coast, *J. Clim.*, *17*, 337–348.

Appleby, P. G., and F. Oldfield (1978), The calculation of Pb-210 dates assuming a constant rate of supply of unsupported Pb–210 to the sediment, *Catena*, *5*, 1–8.

Arzayus, K. M., et al. (2002), Effects of physical mixing on the attenuation of polycyclic aromatic hydrocarbons in estuarine sediments, *Org. Geochem.*, *33*, 1759–1769.

Berner, R. A. (1982), Burial of organic carbon and pyrite sulfur in the modern ocean; Its geochemical and environmental significance, *Am. J. Sci.*, *282*, 451–473.

Bigot, M., et al. (1989), Organic geochemistry of surface sediments from the Huanghe estuary and adjacent Bohai Sea (China), *Chem. Geol.*, *75*, 339–350.

Blackwell, J. A., and J. Tuttle (2004), California fire siege 2003: The story, CA Department of Forestry and Fire Protection report to State of California, 98 pp.

Blair, N. E., et al. (2004), From bedrock to burial: The evolution of particulate organic carbon across coupled watershed–continental margin systems, *Mar. Chem.*, *92*, 141–156.

Bligh, E. G., and W. J. Dyer (1959), A rapid method of total lipid extraction and purification, *Can. J. Biochem. Physiol.*, *37*, 911–917.

Blumer, M., and W. W. Youngblood (1975), Polycyclic aromatic hydrocarbons in soils and recent sediments, *Science*, *188*, 53–55.

Boonyatumanond, R., et al. (2006), Distribution and origins of polycyclic aromatic hydrocarbons (PAHs) in riverine, estuarine, and marine sediments in Thailand, *Mar. Pollut. Bull.*, *52*, 942.

Bouloubassi, I., et al. (2001), Hydrocarbons in surface sediments from the Changjiang (Yangtze River) Estuary, East China Sea, *Mar. Pollut. Bull.*, *42*, 1335–1346.

Carey, A. E., et al. (2005), Organic carbon yields from small, mountainous rivers, New Zealand, *Geophys. Res. Lett.*, *32*, L15404, doi:10.1029/2005GL023159.

Chen, S. J., et al. (2006), Distribution and mass inventories of polycyclic aromatic hydrocarbons and organochlorine pesticides in sediments of the Pearl River Estuary and the northern South China Sea, *Environ. Sci. Technol.*, *40*, 709–714.

Colombo, J. C., et al. (2006), Sources, vertical fluxes, and equivalent toxicity of aromatic hydrocarbons in coastal sediments of the Rio de la Plata Estuary, Argentina, *Environ. Sci. Technol.*, *40*, 734–740.

Countway, R. E., et al. (2003), Polycyclic aromatic hydrocarbon (PAH) distributions and associations with organic matter in surface waters of the York River Estuary, Virginia, *Org. Geochem.*, *34*, 209–224.

Czimczik, C. I., et al. (2002), Effects of charring on mass, organic carbon, and stable carbon isotope composition of wood, *Org. Geochem.*, *33*, 1207–1223.

Czimczik, C. I., et al. (2003), How surface fire in Siberian Scots pine forests affects soil organic carbon in the forest floor: Stocks, molecular structure, and conversion to black carbon (charcoal), *Global Biogeochem. Cycles*, *17*(1), 1020, doi:10.1029/2002GB001956.

Dahlen, M. Z., et al. (1990), Late quaternary history of the Ventura Mainland Shelf, California, *Mar. Geol.*, *94*, 317–340.

Dickhut, R. M., and K. E. Gustafson (1995), Atmospheric inputs of selected polycyclic aromatic hydrocarbons and polychlorinated biphenyls to southern Chesapeake Bay, *Mar. Pollut. Bull.*, *30*, 385–396.

Doong, R., and Y. Lin (2004), Characterization and distribution of polycyclic aromatic hydrocarbon contaminations in surface sediment and water from Gao-ping River, Taiwan, *Water Res.*, *38*, 1733.

Dorman, C. E., and C. D. Winant (2000), The structure and variability of the marine atmosphere around the Santa Barbara Channel, *Mon. Weather Rev.*, *128*, 261.

Drake, D. E., et al. (1972), Sediment transport on the Santa Barbara-Oxnard Shelf, Santa Barbara Channel, CA, in *Shelf sediment transport: Process and pattern*, edited by D. J. P. Swift et al., pp. 307–331, Dowden, Hutchinson & Ross, Inc., Stroudsburg, PA.

Elias, V. O., et al. (2001), Evaluating levoglucosan as an indicator of biomass burning in Carajas, Amazonia: A comparison to the charcoal record, *Geochim. Cosmochim. Acta*, *65*, 267–272.

Evans, R. J., and T. A. Milne (1987), Molecular characterization of the pyrolysis of biomass, *Energy & Fuels*, *1*, 123–137.
Florsheim, J. L., et al. (1991), Fluvial sediment transport in response to moderate storm flows following chaparral wildfire, Ventura County, southern California, *Geol. Soc. Am. Bull.*, *103*, 504–511.
Garcia-Falcon, M. S., et al. (2006), Evolution of the concentrations of polycyclic aromatic hydrocarbons in burnt woodland soils, *Environ. Sci. Technol.*, *40*, 759–763.
Giovannini, G., and S. Lucchesi (1997), Modifications induced in soil physico-chemical parameters by experimental fires at different intensities, *Soil Sci.*, *162*, 479–486.
Goni, M. A., and S. Montgomery (2000), Alkaline CuO oxidation with a microwave digestion system: Lignin analyses of geochemical samples, *Analytical Chem.*, *72*, 3116–3121.
Goni, M. A., et al. (1997), Source and contribution of terrigenous organic carbon to surface sediments in the Gulf of Mexico, *Nature*, *389*, 275–278.
Gonzalez-Perez, J. A., et al. (2004), The effect of fire on soil organic matter-a review, *Environ. Int.*, *30*, 855–870.
Gordon, E. S., and M. A. Goni (2004), Controls on the distribution and accumulation of terrigenous organic matter in sediments from the Mississippi and Atchafalaya River margin, *Mar. Chem.*, *92*, 331–352.
Guzzella, L., and A. DePaolis (1994), Polycyclic aromatic hydrocarbons in sediments of the Adriatic Sea, *Mar. Pollut. Bull.*, *28*, 159–165.
Guzzella, L., et al. (2005), Evaluation of the concentration of HCH, DDT, HCB, PCB and PAH in the sediments along the lower stretch of Hugli estuary, West Bengal, northeast India, *Environ. Int.*, *31*, 523–534.
Hao, W. M., and M. H. Liu (1994), Spatial and temporal distribution of tropical biomass burning, *Global Biogeochem. Cycles*, *8*, 495–503.
Harris, D., et al. (2001), Acid fumigation of soils to remove carbonates prior to total organic carbon or C-13 isotopic analysis, *Soil Sci. Soc. Am. J.*, *65*, 1853–1856.
Hedges, J. I., and J. R. Ertel (1982), Characterization of lignin by gas capillary chromatography of cupric oxide oxidation products, *Analytical Chem.*, *54*, 174–178.
Hedges, J. I., and R. G. Keil (1995), Sedimentary organic matter preservation: an assessment and speculative synthesis, *Mar. Chem.*, *49*, 81–115.
Hedges, J. I., and D. C. Mann (1979), The lignin geochemistry of marine sediments from the southern Washington coast, *Geochim. Cosmochim. Acta*, *43*, 1809–1818.
Inman, D. L., and S. A. Jenkins (1999), Climate change and the episodicity of sediment flux of small California rivers, *J. Geol.*, *107*, 251–270.
Jiang, C., et al. (1998), Polycyclic aromatic hydrocarbons in ancient sediments and their relationships to palaeoclimate, *Organic Geochem.*, *29*, 1721.
Johansen, M. P., et al. (2001), Post-fire runoff and erosion from rainfall simulation: Contrasting forests with shrublands and grasslands, *Hydrol. Processes*, *15*, 2953–2965.
Kao, S. J., and K. K. Liu (1996), Particulate organic carbon export from a subtropical mountainous river (Lanyang Hsi) in Taiwan, *Limnol. Oceanogr.*, *41*, 1749–1757.
Kao, S. J., et al. (2006), Efficient trapping of organic carbon in sediments on the continental margin with high fluvial sediment input off southwestern Taiwan, *Cont. Shelf Res.*, *26*, 2520–2537.
Keller, E. A., et al. (1997), Hydrological response of small watersheds following the southern California Painted Cave fire of June 1990, *Hydrol. Processes*, *11*, 401–414.
Killops, S. D., and M. S. Massoud (1992), Polycyclic aromatic hydrocarbons of pyrolytic origin in ancient sediments: Evidence for Jurassic vegetation fires, *Org. Geochem.*, *18*, 1–7.
Kim, G. B., et al. (1999), Distribution and sources of polycyclic aromatic hydrocarbons in sediments from Kyeonggi Bay, Korea, *Mar. Pollut. Bull.*, *38*, 7.
Kim, E. J., et al. (2003), Effects of forest fire on the level and distribution of PCDD/Fs and PAHs in soil, *Sci. Environ.*, *311*, 177–189.
Kolpack, R. L., and D. E. Drake (1984), Transport of clays in the eastern part of the Santa-Barbara Channel, California, *Geo-Mar. Lett.*, *4*, 191–196.
Komada, T., et al. (2004), Oceanic export of relict carbon by small mountainous rivers, *Geophys. Res. Lett.*, *31*, L07504, doi:10.1029/2004GL019512.
Komada, T., et al. (2005), Sedimentary rocks as sources of ancient organic carbon to the ocean: An investigation through delta C-14 and delta C-13 signatures of organic compound classes, *Global Biogeochem. Cycles*, *19*, GB2017, doi:10.1029/2004GB002347.
Laflamme, R. E., and R. A. Hites (1978), The global distribution of polycyclic aromatic hydrocarbons in recent sediments, *Geochim. Cosmochim. Acta*, *42*, 289–303.
Lave, J., and D. Burbank (2004), Denudation processes and rates in the Transverse Ranges, southern California: Erosional response of a transitional landscape to external and anthropogenic forcing, *J. Geophys. Res.*, *109*, F01006, doi:10.1029/2003JF000023.
Leithold, E. L., and R. S. Hope (1999), Deposition and modification of a flood layer on the northern California shelf: Lessons from and about the fate of terrestrial particulate organic carbon, *Mar. Geol.*, *154*, 183–195.
Leithold, E. L., et al. (2005), Sedimentation and carbon burial on the northern California continental shelf: The signatures of land-use change, *Cont. Shelf Res.*, *25*, 349–371.
Leithold, E. L., et al. (2006), Geomorphologic controls on the age of particulate organic carbon from small mountainous and upland rivers, *Global Biogeochem. Cycles*, *20*, GB3022, doi:10.1029/2005GB002677.
Li, B. (2000), The distribution of *n*-alkanes and PAHs in sediments of Bohai and Yellow Sea, Ms.D. Thesis, p. 89.
Lipiatou, E., and A. Saliot (1991), Fluxes and transport of anthropogenic and natural polycyclic aromatic hydrocarbons in the western Mediterranean Sea, *Mar. Chem.*, *32*, 51–71.
Lohman, D. J., et al. (2007), ENVIRONMENT: The burning issue, *Science*, *316*, 376.
Luo, X. J., et al. (2006), Polycyclic aromatic hydrocarbons in suspended particulate matter and sediments from the Pearl River Estuary and adjacent coastal areas, China, *Environ. Pollut.*, *139*, 9–20.
Lynch, J. A., et al. (2004), Charcoal production, dispersal, and deposition from the Fort Providence experimental fire: Interpreting fire regimes from charcoal records in boreal forests, *Can. J. For. Res. -Revue Canadienne De Recherche Forestiere*, *34*, 1642–1656.
Magi, E., et al. (2002), Distribution of polycyclic aromatic hydrocarbons in the sediments of the Adriatic Sea, *Environ. Pollut.*, *119*, 91.
Masiello, C. A., and E. R. M. Druffel (2001), Carbon isotope geochemistry of the Santa Clara River, *Global Biogeochem. Cycles*, *15*, 407–416, doi:10.1029/2000GB001290.
McGrath, T., et al. (2001), An experimental investigation into the formation of polycyclic-aromatic hydrocarbons (PAH) from pyrolysis of biomass materials, *Fuel*, *80*, 1787.
Mensing, S. A., et al. (1999), A 560-year record of Santa Ana fires reconstructed from charcoal deposited in the Santa Barbara Basin, California, *Quat. Res.*, *51*, 295–305.
Mertes, L. A. K., and J. A. Warrick (2001), Measuring flood output from 110 coastal watersheds in California with field measurements and SeaWiFS, *Geology*, *29*, 659–662.
Miller, N. L., and N. J. Schlegel (2006), Climate change projected fire weather sensitivity: California Santa Ana wind occurrence, *Geophys. Res. Lett.*, *33*, L15711, doi:10.1029/2006GL025808.
Milliman, J. D., and J. P. M. Syvitski (1992), Geomorphic/Tectonic control of sediment discharge to the ocean-The importance of small mountainous rivers, *J. Geol.*, *100*, 525–544.
Mitra, S., et al. (2000), Terrestrially derived dissolved organic matter in the Chesapeake Bay and the Middle Atlantic Blight, *Geochim. Cosmochim. Acta*, *64*, 3547–3557.
Moody, J. A., and D. A. Martin (2001), Initial hydrologic and geomorphic response following a wildfire in the Colorado Front Range, *Earth Surf. Processes Landforms*, *26*, 1049–1070.
Mount, J. F. (1995), *California rivers and streams: The conflict between fluvial processes and land use*, University of California Press, Berkeley, CA, 359 pp.
NAS (2001), National Academy of Sciences: Climate change science: An analysis of some key questions, in *National Academy Press*, Washington DC, 28 pp.
Olivella, M. A., et al. (2006), Distribution of polycyclic aromatic hydrocarbons in riverine waters after Mediterranean forest fires, *Sci. Total Environ.*, *355*, 156–166.
Onstad, G. D., et al. (2000), Sources of particulate organic matter in rivers from the continental USA: Lignin phenol and stable carbon isotope compositions, *Geochim. Cosmochim. Acta*, *64*, 3539–3546.
Oros, D. R., et al. (2002), Organic tracers from wild fire residues in soils and rain/river wash-out, *Water Air Soil Pollut.*, *137*, 203–233.
Otto, A., et al. (2006), Characterization and quantification of biomarkers from biomass burning at a recent wildfire site in northern Alberta, Canada, *Appl. Geochem.*, *21*, 166–183.
Overton, E. B., et al. (2004), Historical polycyclic aromatic and petrogenic hydrocarbon loading in northern central Gulf of Mexico shelf sediments, *Mar. Pollut. Bull.*, *49*, 557–563.
Ozretich, R. J., and W. P. Schroeder (1986), Determination of selected neutral priority organic pollutants in marine sediment, tissue, and reference materials utilizing bonded-phase sorbents, *Analytical Chem.*, *58*, 2041–2048.
Prahl, F. G., and R. Carpenter (1983), Polycyclic aromatic hydrocarbon (PAH)-phase associations in Washington coastal sediment, *Geochim. Cosmochim. Acta*, *47*, 1013–1023.
Pyne, S. J. (1997), *Fire in America*, University of Washington Press, Seattle, WA, 654 pp.

Qiu, Y. J., et al. (1991), Nonaromatic hydrocarbons in suspended matter from Changjiang (Yangtse River) Estuary - Their characterization and variation in winter and summer (low-flow and high-flow) conditions, *Estuarine Coastal Shelf Sci.*, *33*, 153–174.

Ramdahl, T. (1983), Retene-A molecular marker of wood combustion in ambient air, *Nature*, *306*, 580–583.

Ramdahl, T., et al. (1982), Chemical and biological characterization of emissions from small residential stoves burning wood and charcoal, *Chemosphere*, *11*, 601–611.

Rulli, M. C., and R. Rosso (2005), Modeling catchment erosion after wildfires in the San Gabriel Mountains of southern California, *Geophys. Res. Lett.*, *32*, L19401, doi:10.1029/2005GL023635.

Rumpel, C., et al. (2006), Preferential erosion of black carbon on steep slopes with slash and burn agriculture, *Catena*, *65*, 30.

Sarmiento, J., and N. Gruber (2002), Sinks for anthropogenic carbon, *Phys. Today*, *55*, 30–34.

Schauer, J. J., et al. (2001), Measurement of emissions from air pollution sources. 3. C-1 to C-29 organic compounds from fireplace combustion of wood, *Environ. Sci. Technol.*, *35*, 1716–1728.

Schimmelmann, A., and M. J. Tegner (1991), Historical oceanographic events reflected in C-13/C-12 ratio of total organic carbon in laminated Santa Barbara basin sediment, *Global Biogeochem. Cycles*, *5*, 173–188, doi:10.1029/1991GB00382.

Schwalbach, J. R., and D. S. Gorsline (1985), Holocene sediment budgets for the basins of the California Continental Borderland, *J. Sediment. Res.*, *55*, 829–842.

Scott, K. M., and R. P. Williams (1978), Erosion and sediment yield in the Transverse Ranges, southern California, USGS Paper 1030, Palo Alto, CA, 37 pp.

Shafizadeh, F. (1982), Introduction to pyrolysis of biomass, *J. Analytical Appl. Pyrolysis*, *3*, 283–305.

Shakesby, R. A., and S. H. Doerr (2006), Wildfire as a hydrological and geomorphological agent, *Earth Sci. Rev.*, *74*, 269–307.

Sigman, D. M., and E. A. Boyle (2000), Glacial/Interglacial variations in atmospheric carbon dioxide, *Nature*, *407*, 859–869.

Silliman, J. E., et al. (2001), A hypothesis for the origin of perylene based on its low abundance in sediments of Green Bay, Wisconsin, *Chem. Geol.*, *177*, 309–322.

Simoneit, B. R. T. (2002), Biomass burning-A review of organic tracers for smoke from incomplete combustion, *Appl. Geochem.*, *17*, 129–162.

Simoneit, B. R. T., and V. O. Elias (2001), Detecting organic tracers from biomass burning in the atmosphere, *Mar. Pollut. Bull.*, *42*, 805–810.

Simoneit, B. R. T., et al. (1999), Levoglucosan, a tracer for cellulose in biomass burning and atmospheric particles, *Atmos. Environ.*, *33*, 173–182.

Sommerfield, C. K., and C. A. Nittrouer (1999), Modern accumulation rates and a sediment budget for the Eel shelf: A flood-dominated depositional environment, *Mar. Geol.*, *154*, 227.

Sommerfield, C. K., et al. (1999), Be-7 as a tracer of flood sedimentation on the northern California continental margin, *Cont. Shelf Res.*, *19*, 335–361.

Thorton, S. E. (1984), Basin model for hemipelagic sedimentation in a tectonically active continental margin: Santa Barbara Basin, Calfornia Continental Borderland, in *Fine grained sediments: Deep-water processes and facies*, edited by D. A. V. Stow and D. J. W. Piper, pp. 395–415, Blackwell Scientific Publications, Oxford, UK.

Walsh, J. J. (1991), Importance of continental margins in the marine biogeochemical cycling of carbon and nitrogen, *Nature*, *350*, 53–55.

Warrick, J. A. (2002), Short-term (1997–2000) and long-term (1928–2000) observations of river water and sediment discharge to the Santa Barbara Channel, California, PhD Dissertation, University of California, Santa Barbara, 337 pp.

Warrick, J. A., and J. D. Milliman (2003), Hyperpycnal sediment discharge from semiarid southern California rivers: Implications for coastal sediment budgets, *Geology*, *31*, 781–784.

Warrick, J. A., and D. Rubin (2007), Suspended-sediment rating curve response to urbanization and wildfire, Santa Ana River, California, *J. Geophys. Res.*, *112*, F02018, doi:10.1029/2006JF000662.

Warrick, J. A., et al. (2004), A conceptual model for river water and sediment dispersal in the Santa Barbara Channel, California, *Cont. Shelf Res.*, *24*, 2029–2043.

Warrick, J. A., et al. (2005), Nutrient contributions to the Santa Barbara Channel, California, from the ephemeral Santa Clara River, *Estuarine Coastal Shelf Sci.*, *62*, 559–574.

Wollast, R. (1998), Evaluation and comparison of the global carbon cycles in the coastal zone and in the open ocean, in *The Sea: The Global Coastal Ocean*, *10*, edited by K. H. Bring, A. R. Anderson, pp. 213–252, Wiley and Sons, New York.

Yang, G. P. (2000), Polycyclic aromatic hydrocarbons in the sediments of the South China Sea, *Environ. Pollut.*, *108*, 163.

Yunker, M. B., et al. (1996), Polycyclic aromatic hydrocarbon composition and potential sources for sediment samples from the Beaufort and Barents seas, *Environ. Sci. Technol.*, *30*, 1310–1320.

Yunker, M. B., et al. (2002), Sources and significance of alkane and PAH hydrocarbons in Canadian arctic rivers, *Estuarine Coastal Shelf Sci.*, *55*, 1–31.

C. R. Alexander, Skidaway Institute of Oceanography, 10 Ocean Science Circle, Savannah, GA 31411, USA.

G. B. Hunsinger, Department of Geological Sciences and Environmental Studies, Binghamton University, Binghamton, NY 13902-6000, USA.

S. Mitra, East Carolina University, Department of Geological Sciences, 101 Graham Building, Greenville, NC 27858, USA. (mitras@ecu.edu)

J. A. Warrick, USGS Pacific Science Center, 400 Natural Bridges Drive, Santa Cruz, CA 95060, USA.